 Volume 7, Issue 1, (Page 15-37)
ISSN: 2709-0248

Comparative Analysis of Lateral Capacity between Open-Frame and Infill-Frame Systems in a Four-Story Reinforced Concrete Building Using Pushover Analysis

Nyoman Gede Rio Saputra[1], Made Sukrawa[1], Ida Ayu Made Budiwati[1]
[1]Master's Degree Program in Civil Engineering, Faculty of Engineering, Udayana University, Denpasar, Indonesia

Abstract

This study aims to compare the lateral capacity and seismic performance of open-frame (OF) and infill-frame (IF) configurations in an existing four-story reinforced concrete residential building in Badung, Bali. A three-dimensional structural model was developed using SAP2000, with identical geometry, material properties, and loading conditions for both configurations. The OF model excluded the lateral contribution of masonry infill, whereas the IF model incorporated existing infill walls using diagonal compression struts. Nonlinear static pushover analysis was conducted to evaluate base-shear capacity, displacement response, interstory drift, and structural performance. The results show that the IF model achieved higher performance-point base shear than the OF model, increasing from 42,144 to 42,855 kN in the X direction and from 43,825 to 44,788 kN in the Y direction. Performance-point displacement also decreased from 98.421 to 94.399 mm in X and from 93.171 to 91.261 mm in Y. Incorporating infill walls reduced interstory drift by approximately 36–58% and improved lateral stiffness, while both configurations remained within the Immediate Occupancy performance level. However, the relatively similar pushover curves indicate that the contribution of infill walls to overall lateral capacity remains limited because of substantial wall openings. The findings demonstrate that infill modeling provides measurable but moderate improvements in structural seismic performance.

Keywords: Infill Frame; Open Frame; Lateral Capacity; Pushover Analysis; Seismic Performance

Received : July 17, 2026
Received in Revised: August 12, 2026
Accepted: September 1, 2026

Introduction

Seismic performance evaluation has become an essential component of structural engineering, particularly for reinforced concrete buildings located in regions exposed to significant earthquake hazards. Contemporary seismic assessment increasingly emphasizes not only structural strength but also stiffness, deformation capacity, ductility, energy dissipation, and the progression of damage under increasing earthquake demand. Performance-based seismic design and assessment provide a framework for evaluating structural behavior across different performance objectives and inelastic response conditions (Sattar et al., 2021; Badal & Sinha, 2022). For existing buildings, this approach is particularly important because the actual structural configuration may differ from the simplified assumptions adopted during the original design or analytical modeling. Recent studies have demonstrated that nonlinear assessment methods can provide a more comprehensive understanding of the capacity and expected performance of reinforced concrete structures than conventional elastic procedures alone (Güneş et al., 2021; Ali & Sanghai, 2021).

DOI: https://doi.org/10.47667/ijpasr.v7i1.488

Volume 7, Issue 1, (Page 15-37)
ISSN: 2709-0248

Reinforced concrete moment-resisting frames are widely used as primary structural systems for resisting lateral earthquake loads. In an open-frame configuration, lateral resistance is primarily provided by the flexural interaction of beams, columns, and beam-column connections. The seismic response of these systems is strongly influenced by member stiffness, strength hierarchy, ductility, and the development of appropriate plastic mechanisms. Recent performance-based studies of reinforced concrete frames have emphasized the importance of controlling structural damage and maintaining an appropriate strength hierarchy under increasing lateral demand (Sattar et al., 2021; Badal & Sinha, 2022). Numerical investigations have also demonstrated that nonlinear static procedures can be effectively used to identify lateral strength, displacement capacity, yielding characteristics, and structural performance levels of reinforced concrete buildings (Ali & Sanghai, 2021; Hasibuan & Prayuda, 2025). Consequently, evaluating the nonlinear lateral response of reinforced concrete frames is particularly important when assessing existing buildings subjected to seismic demand.

Actual reinforced concrete buildings, however, rarely consist solely of bare structural frames. Masonry walls are commonly installed between beams and columns as interior partitions and exterior enclosures. Although these walls are generally classified as nonstructural components because they do not carry the primary gravity loads, their interaction with the surrounding reinforced concrete frame can significantly modify the seismic response of the building. Experimental and numerical studies conducted in recent years have consistently demonstrated that masonry infills can increase the initial stiffness, lateral strength, and energy dissipation of reinforced concrete frames compared with bare-frame configurations (Wang et al., 2021; Blasi et al., 2021; Shendkar et al., 2022). Experimental cyclic tests have similarly shown that the presence of infill walls changes the mechanical response of reinforced concrete frames and increases their horizontal resistance and stiffness (Wang et al., 2021; Khan et al., 2021).

The contribution of masonry infills is nevertheless strongly dependent on their mechanical properties, configuration, and interaction with the surrounding frame. Numerical investigations have shown that the constitutive representation selected for masonry infill can substantially affect the predicted global strength, stiffness, and energy dissipation of reinforced concrete buildings (Gaetani d'Aragona et al., 2021). Similarly, parametric analyses indicate that the distribution of masonry infills can significantly influence the global seismic response and damage characteristics of reinforced concrete frames (Pallaes et al., 2021; Messaoudi et al., 2022). Experimental research has also demonstrated that the position and stiffness of infill panels affect the seismic response of reinforced concrete frames, indicating that infill walls cannot be treated as mechanically irrelevant components during seismic assessment (Milijaš et al., 2023). These findings emphasize the importance of explicitly considering the presence and distribution of infill walls when evaluating the actual lateral behavior of existing reinforced concrete buildings.

The presence of openings represents another important factor affecting the contribution of masonry infills. Doors and windows interrupt the continuity of masonry panels and reduce the effective area available for transferring compressive forces between the frame and infill. Analytical studies have demonstrated that increasing the size of openings can reduce the lateral strength, stiffness, and ductility of infilled reinforced concrete frames (Kurmi & Haldar, 2022). Furtado et al. (2022) similarly reported that openings modify the global seismic response of infilled reinforced concrete buildings, with larger opening ratios producing reductions in initial stiffness and maximum lateral resistance. Experimental research has confirmed that the location and size of openings influence the strength and stiffness contribution of masonry infills (Messaoudi et al., 2022; Milijaš et al., 2023). More recent experimental evidence has further

DOI: https://doi.org/10.47667/ijpasr.v7i1.488

Volume 7, Issue 1, (Page 15-37)
ISSN: 2709-0248

shown that openings can produce critical wall segments and short-column effects, which may influence the governing failure mechanism of infilled frames (Ou et al., 2024). Therefore, the presence of large openings can explain why an infill-frame system does not necessarily exhibit a proportional increase in global lateral capacity despite the additional stiffness provided by masonry walls.

The interaction between masonry infills and reinforced concrete frames is commonly represented using equivalent diagonal strut models in nonlinear structural analysis. This approach allows the lateral contribution of masonry panels to be incorporated into numerical models without requiring a detailed representation of every masonry component. Akan et al. (2022) demonstrated that simplified pushover procedures incorporating the axial resistance of equivalent infill struts can effectively reproduce the lateral response of infilled reinforced concrete frames. Similarly, Etemadi and Balkaya (2024) used equivalent diagonal struts to represent masonry panels and demonstrated that infills can substantially modify the displacement demand of reinforced concrete frames. Recent numerical investigations have also emphasized the importance of accurately representing local frame-infill interaction because infill walls can modify internal force distributions within surrounding structural members (Etemadi & Balkaya, 2024). These findings support the use of a diagonal-strut representation when comparing open-frame and infill-frame configurations.

Pushover analysis provides an appropriate nonlinear approach for investigating the difference in lateral capacity between these structural configurations. The method produces a capacity curve describing the relationship between base shear and roof or control-node displacement as lateral loading progressively increases. This curve provides information regarding initial stiffness, yielding behavior, maximum lateral resistance, displacement capacity, and the progression of structural response toward inelastic conditions. Recent studies have applied pushover analysis to evaluate reinforced concrete buildings and infilled frames, demonstrating its usefulness for identifying performance points and comparing alternative structural configurations (Akan et al., 2022; Messaoudi et al., 2022; Ou et al., 2024). More recent computational developments have also demonstrated that simplified models can reproduce key aspects of the global lateral response, torsional behavior, and collapse mechanisms of masonry-infilled reinforced concrete buildings (Angelucci et al., 2025).

Although previous studies have established that masonry infills generally increase stiffness and lateral resistance, the magnitude of this contribution remains dependent on the actual configuration of the building. Studies considering openings, irregular infill distributions, and different infill properties have demonstrated that the response of an infill-frame system cannot be generalized solely from the presence of masonry walls (Shendkar et al., 2022; Furtado et al., 2022; Messaoudi et al., 2022). Experimental evidence further indicates that infilled frames may experience lower drift demands than bare frames, although the presence of infills can also influence deformation capacity and failure mechanisms. Recent comparative experimental research found that frames with infill experienced substantially smaller drift demands than otherwise similar bare frames, highlighting the important role of infill in the seismic response of reinforced concrete buildings (Khaled et al., 2024). Consequently, direct comparison of equivalent open-frame and infill-frame models using the same building geometry and loading conditions remains important for understanding the actual contribution of existing masonry infills.

In this context, the present study investigates an existing four-story reinforced concrete residential building in Badung, Bali, designed as a Special Moment Resisting Frame. Two

DOI: https://doi.org/10.47667/ijpasr.v7i1.488

Volume 7, Issue 1, (Page 15-37)
ISSN: 2709-0248

three-dimensional structural configurations are developed using SAP2000. The first configuration represents an open-frame system in which the structural contribution of masonry infills is excluded, while the second represents an infill-frame system in which existing masonry walls are incorporated through diagonal strut elements. Both configurations are subjected to nonlinear static pushover analysis under consistent structural and seismic conditions. The comparison focuses on the resulting capacity curves, base-shear capacity, displacement response, interstory drift, and performance points. The objective is to determine the extent to which the existing infill walls modify the lateral capacity of the four-story reinforced concrete building. This comparison is particularly relevant because the investigated building contains infill panels with substantial openings, which may limit the contribution of masonry walls to the global lateral resistance. The study therefore provides a direct comparative assessment of the lateral capacity difference between open-frame and infill-frame systems based on pushover analysis.

Accordingly, this study aims to compare the lateral capacity of a four-story reinforced concrete building with open-frame and infill-frame configurations based on pushover analysis. The findings are expected to provide a more representative understanding of how modeling assumptions concerning masonry infill affect the estimated lateral capacity of reinforced concrete buildings.

Methods

Research Design

This study employed a comparative numerical analysis to investigate the difference in lateral capacity between open-frame and infill-frame systems in a four-story reinforced concrete building. The analysis was performed using a three-dimensional structural model developed in SAP2000. Two structural configurations were established using identical building geometry, structural dimensions, material properties, and loading conditions. The first configuration represented an open-frame (OF) system in which the lateral contribution of masonry infill walls was not considered. The second configuration represented an infill-frame (IF) system in which the existing masonry infill walls were incorporated into the structural model. Both models were subsequently subjected to nonlinear static pushover analysis. The resulting capacity curves were compared primarily in terms of base shear and structural displacement to determine the difference in lateral capacity between the two systems.

Building Characteristics

The object of analysis was an existing four-story reinforced concrete residential building located in Badung Regency, Bali. The building was classified as Risk Category II and located on hard soil corresponding to Site Class SC. The structural system was designed as a Special Moment Resisting Frame (SRPMK). The ground-floor height was 3.90 m, while the heights of the first, second, and third floors were each 3.60 m, resulting in a total structural height of 14.70 m. The same building geometry was used for both the OF and IF models to ensure that the comparison of lateral capacity was based on the treatment of the infill walls rather than differences in structural configuration. The existing structural plans were used to establish the three-dimensional numerical model and to identify the locations and configurations of the masonry infill walls. The structural plans included infill panels with and without openings, which were retained in the IF model according to their actual arrangement.

Structural Properties and Numerical Modeling

DOI: https://doi.org/10.47667/ijpasr.v7i1.488

Volume 7, Issue 1, (Page 15-37)
ISSN: 2709-0248

The reinforced concrete model used a concrete compressive strength of 24.9 MPa, unit weight of 2,400 kg/m³, elastic modulus of 23,500 MPa, and Poisson's ratio of 0.20. Longitudinal reinforcement had a yield strength of 420 MPa and ultimate strength of 630 MPa, while transverse reinforcement had a yield strength of 280 MPa and ultimate strength of 350 MPa. The elastic modulus of reinforcing steel was 200,000 MPa. These material properties were applied consistently to both structural configurations. The principal column dimensions used in the numerical model are presented in Table 1. The remaining dimensions of beams, slabs, and other structural elements followed the existing structural drawings.

Table 1. Principal Column Dimensions

Column	**Dimension (mm × mm)**
K1	350 × 800
K2	400 × 800
K3	400 × 1350
K6	300 × 300

The three-dimensional structural models were developed in SAP2000. Beams and columns were represented as frame elements, while floor slabs were modeled as shell elements. The OF model was established without considering the stiffness contribution of masonry infill walls. In contrast, the IF model incorporated the existing infill walls according to their actual location and configuration in the building.

Infill-Frame Modeling

The masonry infill walls were incorporated only in the IF model because their contribution was the principal modeling distinction between the two structural systems. The infill walls were modeled in SAP2000 using diagonal compression struts represented by frame elements. The location of each strut followed the actual position of the infill walls, including wall panels with and without openings. This approach allowed the lateral contribution of the masonry infill to be incorporated into the global structural response while maintaining the same reinforced concrete frame geometry used in the OF model. The masonry properties adopted for the strut elements included a masonry compressive strength of 2.97 MPa, mortar compressive strength of 11.22 MPa, wall thickness of 150 mm, unit weight of 596 kg/m³, and elastic modulus of 1,633.5 MPa. The strut width was determined according to the wall geometry and opening configuration.

Table 2. Representative Diagonal Strut Parameters for Ground-Floor Infill Walls

Wall Type	**Wall Height (mm)**	**Wall Length (mm)**	**Opening Height (mm)**	**Opening Length (mm)**	**WscoW_{sco} (mm)**	**WdsW_{ds} (mm)**
WO-1	3000	3075	2750	1700	50.678	132.3
WO-3	3000	2975	850	3025	28.810	1543.7
WO-9	3000	4075	2450	900	18.037	175.8
WC-1-1	3000	4075	—	—	—	1265.1
WC-1-2	3000	3600	—	—	—	1171.5
WC-1-3	3000	3025	—	—	—	1065.1

DOI: https://doi.org/10.47667/ijpasr.v7i1.488

Volume 7, Issue 1, (Page 15-37)
ISSN: 2709-0248

Note: The table presents the representative ground-floor strut calculations available in the source model. Complete calculations for other infill panels are provided in the original structural calculation.

The diagonal struts were modeled to resist compression only. Their mass was not separately assigned because the weight of the masonry walls was assumed to have been transferred to the supporting beams or slabs. Moment releases were applied at both ends of the strut elements, while tensile behavior was prevented by assigning a zero tension limit. Consequently, the IF model captured the compressive contribution of the masonry infill to the lateral response without introducing tensile or flexural resistance from the strut elements.

Loading and Seismic Input

The structural models were subjected to dead, live, wind, rain, and earthquake loads. Gravity loading consisted primarily of structural self-weight, additional dead loads, wall loads, floor finishes, and live loads. Load combinations were established according to SNI 1727:2020. The principal additional dead load on the floor was 126 kg/m², while the residential live load was 1.92 kN/m². Wind and rain loads were also incorporated into the structural model. Earthquake loading was defined according to SNI 1726:2019. The seismic demand used in the nonlinear analysis corresponded to the Maximum Considered Earthquake (MCER), representing an earthquake with a 2% probability of exceedance in 50 years. Site-specific seismic parameters for the hard-soil condition were used to construct the MCER response spectrum

Pushover Analysis Procedure

The lateral capacity of both structural configurations was evaluated using nonlinear static pushover analysis. This method was selected because it provides a capacity curve describing the relationship between base shear and structural displacement as the building undergoes progressively increasing lateral loading. The resulting curves constitute the principal basis for comparing the lateral capacity of the OF and IF systems. Before the lateral loading was applied, the structural models were subjected to gravity loading to establish their initial equilibrium condition. The nonlinear gravity analysis included dead load, additional dead load, live load, and roof live load. The subsequent pushover analysis continued from the final state of the gravity-load analysis. The pushover load was applied as an acceleration load in the X direction using displacement control. Joint 11 in the U1 direction was selected as the control point. The target displacement was defined as 4% of the total structural height. The structural response was recorded at multiple analysis states to capture the progressive nonlinear response until the target displacement or ultimate response was reached.

Lateral Capacity Comparison

The principal dependent variable in this study was lateral capacity, represented by the base-shear capacity obtained from the pushover analysis. The OF and IF models were analyzed using the same structural geometry and general analytical procedure, allowing their capacity responses to be directly compared. The resulting pushover curves were evaluated based on their base-shear magnitude and displacement response. The maximum base shear obtained from each pushover curve was used as the principal indicator for comparing lateral capacity. The comparison also considered the displacement corresponding to the development of the nonlinear response. A higher base shear at a comparable displacement was interpreted as greater lateral resistance. The difference between the two configurations was subsequently expressed as the relative increase or decrease in maximum base shear of the IF model compared with the OF model. The pushover capacity curves were also converted into Acceleration–

DOI: https://doi.org/10.47667/ijpasr.v7i1.488

Volume 7, Issue 1, (Page 15-37)
ISSN: 2709-0248

Displacement Response Spectrum (ADRS) format in SAP2000 to identify the performance point. However, in accordance with the focus of the present article, the performance point was treated as a supporting result rather than the principal outcome. The main analytical comparison remained the difference in the base-shear–displacement capacity curves between the OF and IF systems. The source methodology confirms that the pushover output consists of the base-shear–displacement capacity curve and that the curve can subsequently be converted to ADRS for performance-point determination.

Results and Discussion

The structural response of the four-story reinforced concrete building was evaluated for two structural configurations, namely the open-frame (OF) model and the infill-frame (IF) model. The OF model represents the structural frame without considering the contribution of infill walls, whereas the IF model incorporates the infill walls as additional lateral-stiffness components. Before conducting the nonlinear static analysis, basic structural checks were performed to establish the adequacy of both structural models and to provide a consistent basis for comparing their lateral responses.

Open-Frame Model

Modal Mass Participation Ratio

According to SNI 1726:2019 Article 7.9.1.1, the combined modal mass participation must reach at least 90% of the actual mass in each orthogonal horizontal direction. The modal mass participation results for the OF model are presented in Table 3.

Table 3. Modal Mass Participation Ratio of the OF Model

Case	Static (%)	Dynamic (%)
MODAL	99.99	97.30
MODAL	99.93	90.64

The results indicate that the OF model satisfies the minimum 90% modal mass participation requirement in both orthogonal horizontal directions. The dynamic modal mass participation reaches 97.30% and 90.64%, respectively, indicating that the modal analysis provides sufficient mass participation for subsequent seismic analysis.

Base Shear Check

The base shear obtained from the static and dynamic analyses was evaluated according to SNI 1726:2019 Article 7.9.1.4.1. Before scaling, the dynamic base shear was lower than the static base shear in both directions, as presented in Table 4.

Table 4. Static and Dynamic Seismic Base Shear Results of the OF Model

Base Shear	VS (kN)	VD (kN)	VD ≥ VS	VS/VD
X Direction	1313.088	183.679	Not OK	7.148
Y Direction	1480.280	194.372	Not OK	7.616

The dynamic base shear was 183.679 kN in the X direction and 194.372 kN in the Y direction, compared with static base shear values of 1313.088 kN and 1480.280 kN, respectively. Therefore, the dynamic analysis results required scaling before being used for subsequent structural evaluation.

After scaling, the base shear results are presented in Table 5.

DOI: https://doi.org/10.47667/ijpasr.v7i1.488

Volume 7, Issue 1, (Page 15-37)
ISSN: 2709-0248

Table 5. Static and Dynamic Seismic Base Shear Results after Scaling for the OF Model

Base Shear	VS (kN)	VD (kN)	VD ≥ VS
X Direction	1313.088	1313.640	OK
Y Direction	1480.280	1481.705	OK

After scaling, the dynamic base shear reached 1313.640 kN in the X direction and 1481.705 kN in the Y direction. Both values satisfy the requirement of VD ≥ 100% VS and were therefore used in subsequent structural evaluation.

Interstory Drift

The interstory drift of the OF model was evaluated to determine the relative lateral deformation between floors under seismic loading. The results are presented in Table and Figure.

Table 6. Interstory Drift Check of the OF Model

Floor	Story Height (mm)	Drift X (mm)	Drift Y (mm)	(dX × Cd) (mm)	(dY × Cd) (mm)	Allowable Drift (mm)	X	Y
Floor 4	3600	0.69	1.24	4.40	4.53	24.22	24.92	69.23
Floor 3	3600	5.09	5.77	0.29	0.33	1.61	1.82	69.23
Floor 2	3600	4.80	5.44	1.71	1.99	9.41	10.96	69.23
Floor 1	3900	3.09	3.44	3.09	3.44	16.97	18.95	75.00

The OF model satisfies the allowable interstory drift requirements in both the X and Y directions.

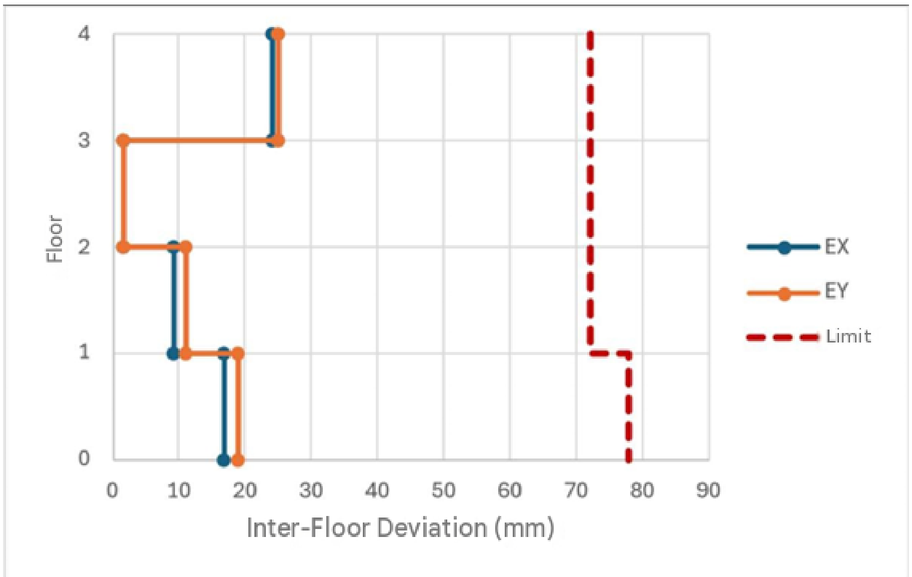

Figure 1. Interstory Drift of the OF Structure

P-Δ Effect

The P-Δ effect was evaluated using the stability coefficient θ. The results for the X and Y directions are presented in Tables.

DOI: https://doi.org/10.47667/ijpasr.v7i1.488

Volume 7, Issue 1, (Page 15-37)
ISSN: 2709-0248

Table 7. P-Delta Effect Check in the X Direction for the OF Model

Floor	Px (kN)	Dx (mm)	Seismic Shear X (kN)	Story Height (mm)	θx	θmax	Check
Floor 4	6125.19	-24.22	2864.59	3600	-0.003	0.09	OK
Floor 3	12250.38	1.61	3158.20	3600	0.000	0.09	OK
Floor 2	18375.57	9.41	3398.22	3600	0.003	0.09	OK
Floor 1	24500.77	16.97	3517.82	3900	0.006	0.09	OK

Table 8. P-Delta Effect Check in the Y Direction for the OF Model

Floor	Py (kN)	Dy (mm)	Seismic Shear Y (kN)	Story Height (mm)	θy	θmax	Check
Floor 4	6125.19	-24.92	2872.54	3600	-0.003	0.09	OK
Floor 3	12250.38	1.82	3162.92	3600	0.000	0.09	OK
Floor 2	18375.57	10.96	3399.81	3600	0.003	0.09	OK
Floor 1	24500.77	18.95	3517.82	3900	0.006	0.09	OK

The stability coefficient θ at all floors remained below the specified limit. Therefore, the P-Δ effect was not significant and did not affect the overall stability of the OF structure.

Soft-Story Irregularity

The soft-story irregularity evaluation of the OF model is presented in Tables 7–10.

Table 9. Soft-Story Irregularity Check in the X Direction for the OF Model

Floor	Shear X (kN)	Drift X (mm)	Stiffness X (kN/m)	70% Check	80% Check	Average
Floor 4	2864.5941	-4.40333	806385.309	None	0.00	None
Floor 3	3158.1951	0.292061	1062077.242	None	215036.08	None
Floor 2	3398.2225	1.711055	1541836.578	None	498256.68	None
Floor 1	3517.8177	3.085922	3067688.052	None	909413.10	None

Table 10. Soft-Story Irregularity Check in the Y Direction for the OF Model

Floor	Shear Y (kN)	Drift Y (mm)	Stiffness Y (kN/m)	70% Check	80% Check	Average
Floor 4	2872.5445	-4.531284	822896.087	None	0	None

DOI: https://doi.org/10.47667/ijpasr.v7i1.488

Volume 7, Issue 1, (Page 15-37)
ISSN: 2709-0248

Floor 3	3162.923	0.330541	1080380.064	None	219438.9565	None
Floor 2	3399.8072	1.993021	1563026.042	None	507540.3069	None
Floor 1	3517.8178	3.444567	3093825.341	None	924347.2515	None

Table 11. Excessive Soft-Story Irregularity Check in the X Direction for the OF Model

Floor	Shear X (kN)	Drift X (mm)	Stiffness X (kN/m)	60% Check	70% Check	Average
Floor 4	2864.5941	-4.40333	806385.309	None	0	None
Floor 3	3158.1951	0.292061	1062077.242	None	188156.5721	None
Floor 2	3398.2225	1.711055	1541836.578	None	435974.5952	None
Floor 1	3517.8177	3.085922	3067688.052	None	795736.4634	None

Table 12. Excessive Soft-Story Irregularity Check in the Y Direction for the OF Model

Floor	Shear Y (kN)	Drift Y (mm)	Stiffness Y (kN/m)	60% Check	70% Check	Average
Floor 4	2872.5445	-4.531284	822896.087	None	0	None
Floor 3	3162.923	0.330541	1080380.064	None	192009.087	None
Floor 2	3399.8072	1.993021	1563026.042	None	444097.7686	None
Floor 1	3517.8178	3.444567	3093825.341	None	808803.845	None

The evaluation indicates that the OF model does not exhibit soft-story irregularity.

Torsional Irregularity

Torsional irregularity was evaluated in both principal directions. The results are presented in Tables.

Table 13. Torsional Irregularity Check in the X Direction for the OF Model

Floor	Max Drift X (mm)	dx (mm)	Min (dx·Cd)/Ie (mm)	Story Drift X Min (mm)	Min Story Drift Y × Cd	Δavg X	1.2Δavg X	1.4Δavg X	Check
Floor 4	0.69	-4.40	-24.218	0.685	-4.403	-24.218	-29.061	-33.905	Torsional
Floor 3	5.089	0.292	1.606	5.089	0.292	1.606	1.927	2.248	No torsion
Floor 2	4.796	1.711	9.410	4.796	1.711	9.410	11.292	13.175	No torsion

DOI: https://doi.org/10.47667/ijpasr.v7i1.488

Floor 1	3.085	3.085	16.972	3.085	3.085	16.972	20.367	23.761	No torsion

Table 14. Torsional Irregularity Check in the Y Direction for the OF Model

Floor	**Max Drift Y (mm)**	**dy (mm)**	**Min (dy·Cd)/Ie (mm)**	**Story Drift Y Min (mm)**	**Min Story Drift X × Cd**	**Δavg Y**	**1.2Δavg Y**	**1.4Δavg Y**	**Check**
Floor 4	1.236	-4.531	-24.922	1.236	-4.531	-24.922	-29.906	-34.890	Torsional
Floor 3	5.768	0.330	1.817	5.768	0.330	1.817	2.181	2.545	No torsion
Floor 2	5.437	1.993	10.961	5.437	1.993	10.961	13.153	15.346	No torsion
Floor 1	3.444	3.444	18.945	3.444	3.444	18.945	22.734	26.523	No torsion

The results indicate torsional irregularity at Floor 4 in both directions. Therefore, linear dynamic analysis was required in accordance with SNI 1726:2019 Article 7.6.

Structural Capacity Check

The PMM capacity ratios of the OF columns were below 1.0.

Table 15. PMM Ratio Check of OF Structural Columns

Frame	**Column Number**	**Ratio**	**Check**
K1	105	0.491	OK!
K1	106	0.467	OK!
K1	85	0.462	OK!
K2	173	0.521	OK!
K2	165	0.515	OK!
K2	77	0.454	OK!
K3	116	0.165	OK!
K3	119	0.160	OK!
K3	120	0.159	OK!
K6	2332	0.733	OK!
K6	2333	0.715	OK!
K6	4403	0.621	OK!

The maximum PMM ratio was 0.733, indicating that the column sections and reinforcement of the OF model satisfied the specified design requirements.

Infill-Frame Model

The IF model was evaluated using the same structural response parameters to provide a consistent comparison with the OF model. In this model, the infill walls were considered as additional components contributing to the lateral stiffness of the structure.

Modal Mass Participation Ratio

Table 16. Modal Mass Participation Ratio of the IF Model

Case	**Static (%)**	**Dynamic (%)**

DOI: https://doi.org/10.47667/ijpasr.v7i1.488

Volume 7, Issue 1, (Page 15-37)
ISSN: 2709-0248

MODAL	99.75	91.02
MODAL	98.98	96.24

The dynamic modal mass participation values of 91.02% and 96.24% satisfy the minimum 90% requirement.

Base Shear Check

Table 17. Static and Dynamic Seismic Base Shear Results of the IF Model

Base Shear	VS (kN)	VD (kN)	VD ≥ VS	VS/VD
X Direction	1636.301	234.745	Not OK	6.971
Y Direction	1809.092	248.411	Not OK	7.283

After scaling, the results are presented in Table.

Table 18. Static and Dynamic Seismic Base Shear Results after Scaling for the IF Model

Base Shear	VS (kN)	VD (kN)	VD ≥ VS
X Direction	1636.301	1636.722	OK
Y Direction	1809.092	1809.657	OK

The scaled dynamic base shear values satisfy the required criterion in both directions.

Interstory Drift

Table 19. Interstory Drift Check of the IF Model

Floor	Story Height (mm)	Drift X (mm)	Drift Y (mm)	(dX × Cd) (mm)	(dY × Cd) (mm)	Allowable Drift (mm)	X	Y
Floor 4	3600	0.51	1.02	4.44	3.76	15.52	13.18	72
Floor 3	3600	4.95	4.79	0.20	0.22	0.69	0.76	72
Floor 2	3600	4.75	4.57	1.73	1.46	6.04	5.10	72
Floor 1	3900	3.02	3.11	3.02	3.11	10.58	10.90	78

The IF model satisfies the allowable interstory drift requirements. Compared with the OF model, the inclusion of infill walls reduces interstory drift by approximately 36–58%, indicating an increase in lateral stiffness.

DOI: https://doi.org/10.47667/ijpasr.v7i1.488

Volume 7, Issue 1, (Page 15-37)
ISSN: 2709-0248

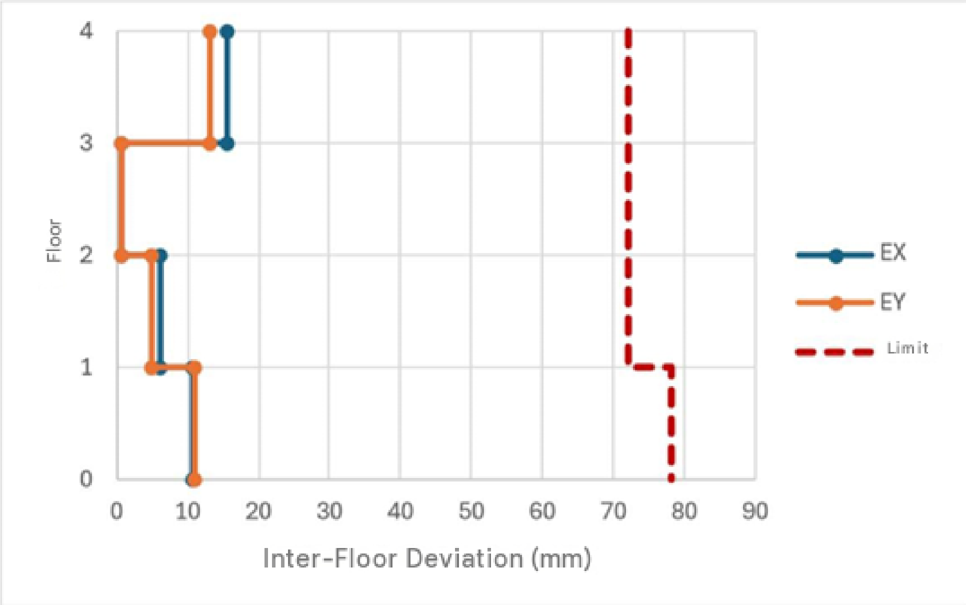

Figure 2. Interstory Drift of the IF Structure

The infill frame structure continues to meet the allowable inter-story drift requirements specified in SNI 1726:2019 (Table 20). Furthermore, a comparison with the response of the OF structure reveals that incorporating infill wall modeling into the IF structure reduces inter-story drift values by approximately 36%–58%, as shown in Figure 3. Thus, it can be concluded that accounting for infill walls in the structural model effectively increases structural stiffness.

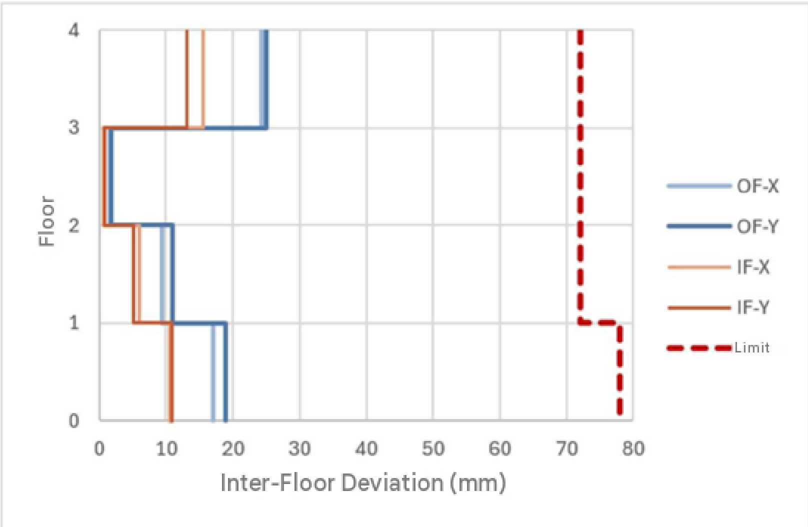

Figure 3. Comparison of Interstory Drift Response of OF and IF

P-Δ Effect

Table 20. P-Delta Effect Check in the X Direction for the IF Model

Floor	**Px (kN)**	**Dx (mm)**	**Seismic Shear X (kN)**	**Story Height (mm)**	**θx**	**θmax**	**Check**
Floor 4	800.23	-15.52	2254.30	3600	-0.00044	0.143	OK

DOI: https://doi.org/10.47667/ijpasr.v7i1.488

Volume 7, Issue 1, (Page 15-37)
ISSN: 2709-0248

Floor 3	7655.08	0.69	1661.06	3600	0.00025	0.143	OK
Floor 2	14663.28	6.04	3317.57	3600	0.00212	0.143	OK
Floor 1	46633.24	10.58	4661.21	3900	0.00776	0.143	OK

Table 21. P-Delta Effect Check in the Y Direction for the IF Model

Floor	**Py (kN)**	**Dy (mm)**	**Seismic Shear Y (kN)**	**Story Height (mm)**	**θy**	**θmax**	**Check**
Floor 4	800.23	-3.764	2279.86	3600	- 0.0001	0.143	OK
Floor 3	7655.08	0.219	1343.79	3600	0.0001	0.143	OK
Floor 2	14663.28	1.457	2937.13	3600	0.0006	0.143	OK
Floor 1	46633.24	3.114	4461.92	3900	0.0024	0.143	OK

The stability coefficients remained below the specified limits in all floors and directions. Therefore, the P-Δ effect was not significant for the overall stability of the IF structure.

Soft-Story Irregularity

Table 22. Soft-Story Irregularity Check in the X Direction for the IF Model

Floor	**Shear X (kN)**	**Drift X (mm)**	**Stiffness X (kN/m)**	**70% Check**	**80% Check**	**Average**
Floor 4	2254.30	-4.44	508251.10	None	0	None
Floor 3	1661.06	0.20	8440370.53	None	406600.88	None
Floor 2	3317.57	1.73	1923007.73	Present	3579448.65	Present
Floor 1	4661.21	3.02	1541404.76	None	2899101.16	Present

Table 23. Soft-Story Irregularity Check in the Y Direction for the IF Model

Floor	**Shear Y (kN)**	**Drift Y (mm)**	**Stiffness Y (kN/m)**	**70% Check**	**80% Check**	**Average**
Floor 4	2279.86	-3.76	605635.89	None	0	None
Floor 3	1343.79	0.22	6150073.25	None	484508.71	None
Floor 2	2937.13	1.46	2015462.34	Present	2702283.66	Present
Floor 1	4461.92	3.11	1433089.45	None	2338979.06	Present

Table 24. Excessive Soft-Story Irregularity Check in the X Direction for the IF Model

DOI: https://doi.org/10.47667/ijpasr.v7i1.488

Floor	Shear X (kN)	Drift X (mm)	Stiffness X (kN/m)	60% Check	70% Check	Average
Floor 4	2254.30	-4.44	508251.10	None	0	None
Floor 3	1661.06	0.20	8440370.53	None	355775.77	None
Floor 2	3317.57	1.73	1923007.73	Present	3132017.57	Present
Floor 1	4661.21	3.02	1541404.76	None	2536713.52	Present

Table 25. Excessive Soft-Story Irregularity Check in the Y Direction for the IF Model

Floor	Shear Y (kN)	Drift Y (mm)	Stiffness Y (kN/m)	60% Check	70% Check	Average
Floor 4	2254.30	-4.44	508251.10	None	0	None
Floor 3	1661.06	0.20	8440370.53	None	355775.77	None
Floor 2	3317.57	1.73	1923007.73	Present	3132017.57	Present
Floor 1	4661.21	3.02	1541404.76	None	2536713.52	Present

The IF model exhibits soft-story irregularity at Floors 1 and 2. This condition is associated with the larger first-story height and the non-uniform distribution of infill walls, which produces a non-uniform vertical stiffness distribution.

Torsional Irregularity

Table 26. Torsional Irregularity Check in the X Direction for the IF Model

Floor	Max Drift X (mm)	dx (mm)	Min (dx·Cd)/Ie (mm)	Story Drift X Min (mm)	Min Story Drift Y × Cd	Δavg X	1.2Δavg X	1.4Δavg X	Check
Floor 4	0.511	-4.43	-15.52	0.511	-4.435	-15.52	-18.62	-21.73	Torsional
Floor 3	4.946	0.197	0.689	4.946	0.197	0.689	0.827	0.964	No torsion
Floor 2	4.749	1.725	6.038	4.749	1.725	6.038	7.246	8.453	No torsion
Floor 1	3.024	3.024	10.584	3.024	3.024	10.584	12.701	14.818	No torsion

Table 27. Torsional Irregularity Check in the Y Direction for the IF Model

Floor	Max Drift Y (mm)	dy (mm)	Min (dy·Cd)/Ie (mm)	Story Drift Y Min (mm)	Min Story Drift X × Cd	Δavg Y	1.2Δavg Y	1.4Δavg Y	Check

DOI: https://doi.org/10.47667/ijpasr.v7i1.488

Volume 7, Issue 1, (Page 15-37)
ISSN: 2709-0248

Floor 4	1.025	-3.76	-13.17	1.025	-3.764	-13.175	-15.810	-18.446	Torsional
Floor 3	4.789	0.219	0.765	4.789	0.219	0.765	0.918	1.071	No torsion
Floor 2	4.571	1.457	5.101	4.571	1.457	5.101	6.121	7.141	No torsion
Floor 1	3.114	3.114	10.897	3.114	3.114	10.897	13.077	15.256	No torsion

Torsional irregularity occurs at Floor 4 in both directions, indicating the need for linear dynamic analysis for the IF structure.

Structural Capacity Check

Table 28. PMM Ratio Check of IF Structural Columns

Frame	Column Number	Ratio	Check
K1	105	0.491	OK!
K1	106	0.468	OK!
K1	85	0.463	OK!
K2	173	0.526	OK!
K2	165	0.520	OK!
K2	77	0.455	OK!
K3	116	0.159	OK!
K3	119	0.158	OK!
K3	120	0.156	OK!
K6	2332	0.737	OK!
K6	2333	0.723	OK!
K6	4403	0.656	OK!

All PMM ratios remain below 1.0. Compared with the OF model, most IF columns show lower PMM ratios, indicating that the infill struts contribute to lateral load resistance and reduce the demand on the columns.

Pushover Capacity and Global Performance

The nonlinear static pushover analysis was conducted to evaluate the global lateral capacity of the OF and IF models. The capacity curve represents the relationship between base shear and lateral displacement. The performance point was determined according to ASCE 41-13 using the Badung Regency MCER earthquake demand spectrum.

Open-Frame Model

The capacity curves and performance points of the OF model in the X and Y directions are presented in Figure 4 and Figure 5, respectively.

DOI: https://doi.org/10.47667/ijpasr.v7i1.488

Volume 7, Issue 1, (Page 15-37)
ISSN: 2709-0248

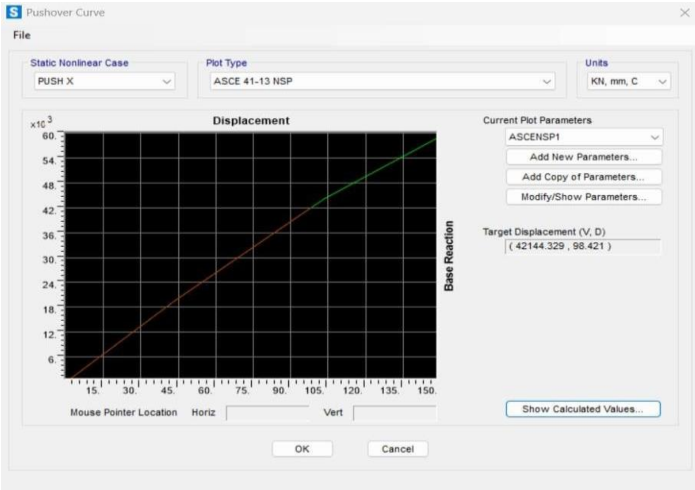

Figure 4. Capacity Curve and Performance Point of Structure OF in the X-direction.

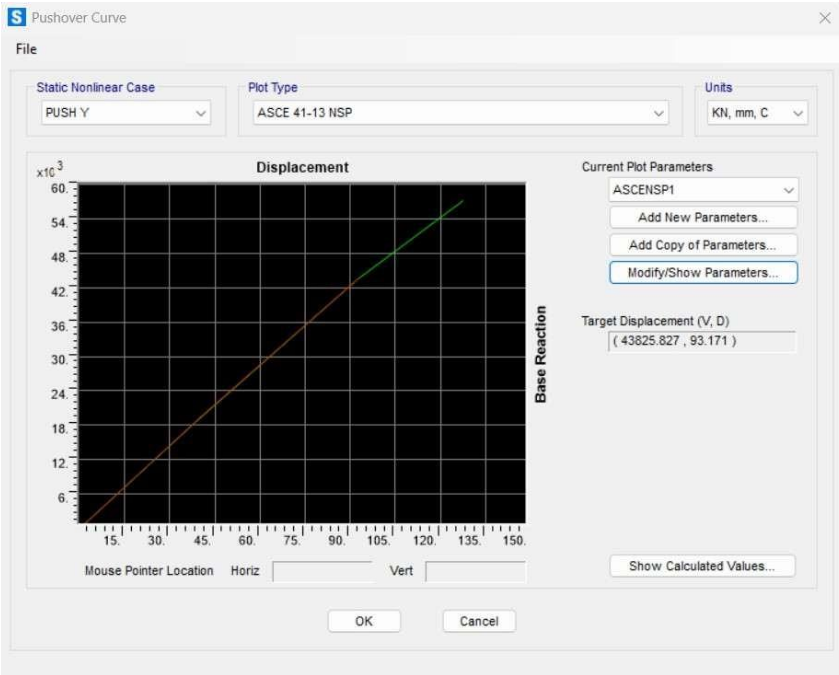

Figure 5. Capacity Curve and Performance Point of OF Structure in Y Direction

The performance point of the OF model in the X direction occurs at (V; D) = (42144 kN; 98.421 mm), while the performance point in the Y direction occurs at (V; D) = (43825 kN; 93.171 mm).

Table 29. Tingkat Kinerja Global Struktur OF

Direction	Structural Height (mm)	Global Drift	Performance Level
X	14700	0.0067	Immediate Occupancy
Y	14700	0.0063	Immediate Occupancy

The OF model reaches the Immediate Occupancy (IO) performance level in both loading directions.

Infill-Frame Model

DOI: https://doi.org/10.47667/ijpasr.v7i1.488

Volume 7, Issue 1, (Page 15-37)
ISSN: 2709-0248

The capacity curves and performance points of the IF model in the X and Y directions are presented in Figure 6 and Figure 7, respectively.

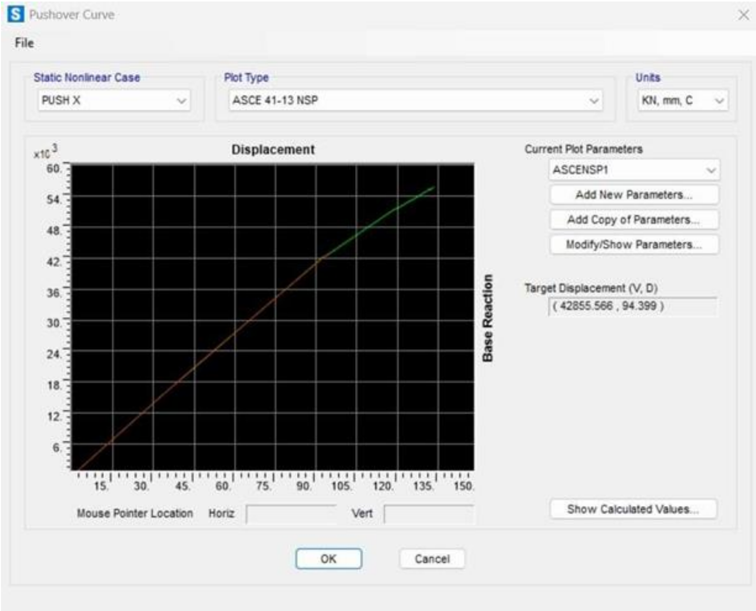

Figure 6. Capacity Curve and Performance Point of IF Structure in the X-direction.

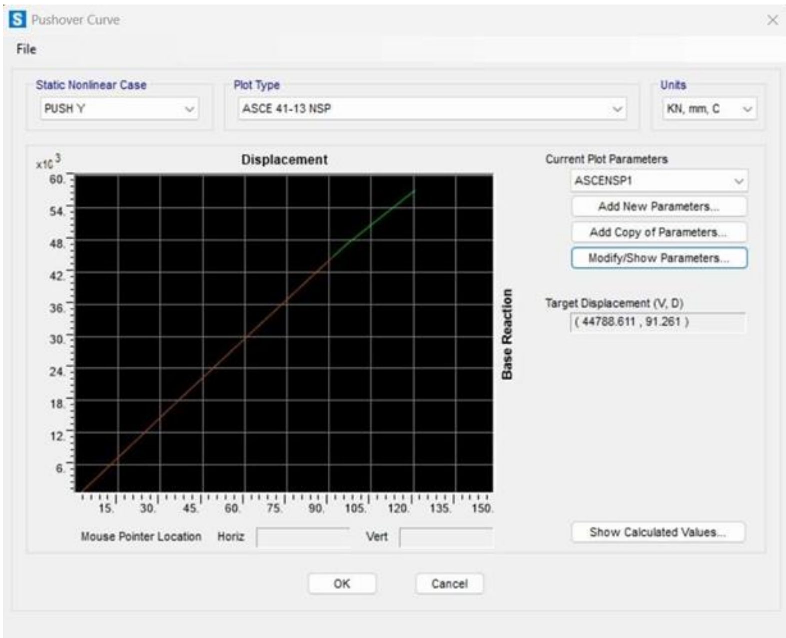

Figure 7. Capacity curve and performance point of the IF structure in the Y-direction.

The performance point of the IF model in the X direction occurs at (V; D) = (42855 kN; 94.399 mm), while the performance point in the Y direction occurs at (V; D) = (44788 kN; 91.261 mm).

Table 30. Global Performance Level of the IF Structure

Direction	Structural Height (mm)	Global Drift	Performance Level
X	14700	0.0064	Immediate Occupancy
Y	14700	0.0062	Immediate Occupancy

DOI: https://doi.org/10.47667/ijpasr.v7i1.488

Volume 7, Issue 1, (Page 15-37)
ISSN: 2709-0248

The IF model also reaches the Immediate Occupancy (IO) performance level in both loading directions.

Comparison of Pushover Capacity between OF and IF Models

The pushover capacity curves of the OF and IF models represent the relationship between base shear and lateral displacement. The original file presents the comparative pushover results in Figure 8 and Figure 9.

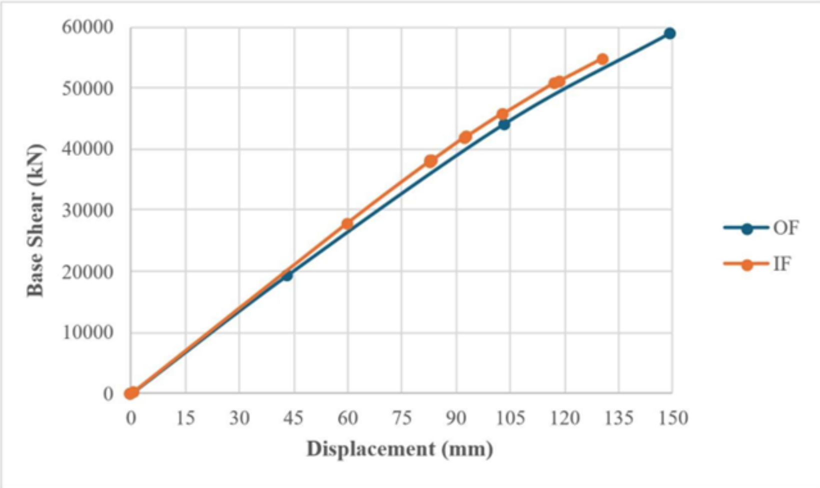

Figure 8. X-direction OF Capacity Curve

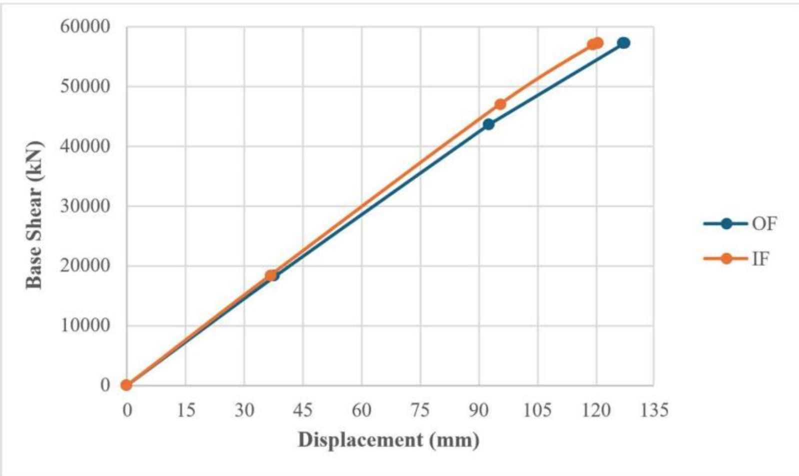

Figure 9. OF Capacity Curve Y Direction

The pushover capacity curves of the OF and IF models exhibit a relatively similar trend, with base shear increasing as lateral displacement increases. The close similarity between the curves indicates that the addition of infill walls does not produce a significant change in the global structural response in the investigated loading directions.

Nevertheless, the IF model consistently exhibits slightly higher base shear values than the OF model. This indicates that the infill walls contribute to increasing the lateral stiffness and lateral capacity of the structure. The increase in base shear is relatively limited because most of the infill walls have large opening ratios, which reduce their effectiveness in forming diagonal compression-strut mechanisms and consequently limit their contribution to global stiffness and lateral capacity.

DOI: https://doi.org/10.47667/ijpasr.v7i1.488

Volume 7, Issue 1, (Page 15-37)
ISSN: 2709-0248

The performance-point results provide a direct numerical comparison of the two structural systems.

Table 31. Comparison of Performance-Point Base Shear and Displacement between the OF and IF Models

Direction	OF V (kN)	IF V (kN)	Difference (kN)	OF D (mm)	IF D (mm)
X	42144	42855	711	98.421	94.399
Y	43825	44788	963	93.171	91.261

The IF model therefore provides an additional 711 kN of performance-point base shear in the X direction and 963 kN in the Y direction. At the same time, the performance-point displacement decreases from 98.421 mm to 94.399 mm in X and from 93.171 mm to 91.261 mm in Y. These results indicate that the infill walls improve both lateral resistance and stiffness, although their contribution to the global capacity remains relatively limited.

Comparison of Lateral Capacity Based on Response Spectrum and Pushover Analysis

The maximum base shear obtained from pushover analysis (Vmax) was compared with the base shear obtained from Response Spectrum analysis (VRS). The Vmax/VRS ratio was used to evaluate the relationship between the lateral capacity obtained from pushover analysis and the seismic force demand obtained from Response Spectrum analysis. The results are presented in Table 32.

Table 32. Comparison of Base Shear Results from Response Spectrum and Pushover Analysis

Model	Direction	VRS (kN)	Vmax Pushover (kN)	Vmax/VRS
OF	X	1313.640	802.921	0.61
OF	Y	1481.705	2696.068	1.82
IF	X	1636.722	831.459	0.51
IF	Y	1809.657	2693.269	1.49

For the OF model, the Vmax/VRS ratio is 0.61 in the X direction and 1.82 in the Y direction. For the IF model, the ratio is 0.51 in the X direction and 1.49 in the Y direction.

In the X direction, the ratios below unity indicate that the maximum base shear obtained from pushover analysis is lower than the base shear obtained from Response Spectrum analysis. Conversely, the ratios above unity in the Y direction indicate that the lateral capacity obtained from pushover analysis is greater than the corresponding seismic force demand. The differences between the X and Y directions are associated with the different stiffness characteristics and structural configurations in the two directions. In the IF model, the non-uniform distribution of infill walls in the X and Y directions also affects the contribution of the diagonal strut elements to structural stiffness and lateral capacity, resulting in different Vmax/VRS ratios.

Summary of the Comparative Lateral Capacity Results

The principal results directly related to the comparison of lateral capacity between the OF and IF systems are summarized in Table 33.

Table 33. Comparative Lateral Capacity Results of the OF and IF Models

Parameter	Open-Frame (OF)	Infill-Frame (IF)
Response Spectrum Base Shear, X (kN)	1313.640	1636.722

DOI: https://doi.org/10.47667/ijpasr.v7i1.488

Volume 7, Issue 1, (Page 15-37)
ISSN: 2709-0248

Response Spectrum Base Shear, Y (kN)	1481.705	1809.657
Performance-Point Base Shear, X (kN)	42144	42855
Performance-Point Base Shear, Y (kN)	43825	44788
Performance-Point Displacement, X (mm)	98.421	94.399
Performance-Point Displacement, Y (mm)	93.171	91.261
Global Drift, X	0.0067	0.0064
Global Drift, Y	0.0063	0.0062
Performance Level, X	Immediate Occupancy	Immediate Occupancy
Performance Level, Y	Immediate Occupancy	Immediate Occupancy
Interstory Drift Reduction	—	36–58%
Vmax/VRS, X	0.61	0.51
Vmax/VRS, Y	1.82	1.49

The results demonstrate that the IF model provides higher performance-point base shear than the OF model in both principal directions. The performance-point base shear increases from 42,144 kN to 42,855 kN in the X direction and from 43,825 kN to 44,788 kN in the Y direction. At the same time, the corresponding performance-point displacement decreases from 98.421 mm to 94.399 mm in X and from 93.171 mm to 91.261 mm in Y.

The reduction in interstory drift of approximately 36–58% further confirms the contribution of the infill walls to lateral stiffness. However, the relatively close pushover capacity curves indicate that the contribution of the infill walls to the overall lateral capacity remains limited. The large opening ratios of the infill walls reduce their effectiveness in developing compression-strut action, resulting in an additional contribution to the existing frame rather than a fundamental change in the global structural response. The comparison with Response Spectrum analysis also demonstrates that the lateral capacity is direction-dependent. In the X direction, both models have Vmax/VRS ratios below unity, whereas in the Y direction both ratios exceed unity. The IF model consequently exhibits a different capacity-demand relationship from the OF model, particularly because of the non-uniform distribution of infill walls and their influence on the lateral stiffness of the structure.

Conclusion

Based on the structural response analysis, both the open-frame (OF) and infill-frame (IF) models satisfy fundamental structural analysis requirements, including modal mass participation, scaled base shear, inter-story drift, and stability against P-Δ effects. The IF model demonstrates superior lateral performance compared to the OF model, evidenced by an increase in performance-point base shear—from 42,144 kN to 42,855 kN in the X-direction and from 43,825 kN to 44,788 kN in the Y-direction—accompanied by a reduction in performance-point displacement from 98.421 mm to 94.399 mm and from 93.171 mm to 91.261 mm, respectively. Modeling the infill walls also reduced inter-story drift by approximately 36–58%, indicating enhanced structural lateral stiffness. Both models remained within the Immediate Occupancy (IO) performance level in both the X and Y directions. However, the similarity of the pushover capacity curves suggests that the infill walls' contribution to the structure's global capacity remains relatively limited; this is primarily due to the large wall opening ratio, which diminishes the effectiveness of the compression strut mechanism. Thus, while the infill walls

DOI: https://doi.org/10.47667/ijpasr.v7i1.488

Volume 7, Issue 1, (Page 15-37)
ISSN: 2709-0248

contribute positively to the structure's lateral stiffness and capacity, they function more as supplementary elements to the existing frame system rather than fundamentally altering the structure's global response characteristics.

Suggestions

Nonlinear analysis can be conducted using the nonlinear time-history analysis method, allowing for a more detailed evaluation of the structure's dynamic behavior under actual earthquake records compared to pushover analysis.Future research could consider variations in the number of building stories, structural configurations, and structural irregularities to gain a more comprehensive understanding of the influence of infill walls on the structure's seismic performance.

References

Ali, S., & Sanghai, S. S. (2021). Seismic vulnerability assessment of reinforced concrete buildings using pushover analysis. *AIP Conference Proceedings, 2417*(1), 020018. https://doi.org/10.1063/5.0072814

Angelucci, G., De Luca, F., De Risi, R., Mollaioli, F., & Spacone, E. (2025). Simplified model for the seismic performance of masonry infilled RC buildings. *Engineering Structures, 342*, 120903. https://doi.org/10.1016/j.engstruct.2025.120903

Akan, Ö. D., O'Reilly, G. J., & Monteiro, R. (2022). Simplified modelling and pushover analysis of infilled frame structures accounting for strut flexibility. *Earthquake Engineering & Structural Dynamics, 51*, 1383–1409. https://doi.org/10.1002/eqe.3620

Badal, P. S., & Sinha, R. (2022). A multi-objective performance-based seismic design framework for building typologies. *Earthquake Engineering & Structural Dynamics*. https://doi.org/10.1002/eqe.3618

Blasi, G., De Luca, F., Perrone, D., Greco, A., & Aiello, M. A. (2021). MID 1.1: Database for characterization of the lateral behavior of infilled frames. *Journal of Structural Engineering, 147*(10). https://doi.org/10.1061/(ASCE)ST.1943-541X.0003117

Etemadi, A., & Balkaya, C. (2024). The role of masonry infills on the interstory drift demand of reinforced concrete frames. *Soil Dynamics and Earthquake Engineering, 180*, 108599. https://doi.org/10.1016/j.soildyn.2024.108599

Furtado, A., Rodrigues, H., & Arêde, A. (2022). Effect of the openings on the seismic response of an infilled reinforced concrete structure. *Buildings, 12*(11), 2020. https://doi.org/10.3390/buildings12112020

Gaetani d'Aragona, M., Polese, M., & Prota, A. (2021). Effect of masonry infill constitutive law on the global response of infilled RC buildings. *Buildings, 11*(2), 57. https://doi.org/10.3390/buildings11020057

Güneş, B., Coşgun, T., Mangır, A., & Sayın, B. (2021). Seismic performance of existing RC framed buildings using pushover analysis method. In *Proceedings/Book chapter on seismic performance assessment of existing reinforced concrete structures*. Springer. https://doi.org/10.1007/978-981-15-8603-3_21

DOI: https://doi.org/10.47667/ijpasr.v7i1.488

Issa, M., Dutu, A., Craifaleanu, I.-G., & Seki, M. (2021). Numerical analysis of a reinforced concrete frame with masonry infill under seismic loading. *CONSTRUCȚII Journal, 1*, 29–38.

Khan, N. A., Bergami, A. V., Nuti, C., Monti, G., Vailati, M., & Briseghella, B. (2021). Seismic performance of Pakistani-technique infilled reinforced concrete frames. In *Proceedings of the 8th International Conference on Computational Methods in Structural Dynamics and Earthquake Engineering (COMPDYN 2021)*.

Kurmi, P., & Haldar, P. (2022). Modeling of opening for realistic assessment of infilled RC frame buildings. *Structures, 41*, 1700–1709. https://doi.org/10.1016/j.istruc.2022.05.110

Messaoudi, A., Chebili, R., Mohamed, H., & Rodrigues, H. (2022). Influence of masonry infill wall position and openings in the seismic response of reinforced concrete frames. *Applied Sciences, 12*(19), 9477. https://doi.org/10.3390/app12199477

Milijaš, A., Marinković, M., Butenweg, C., & Klinkel, S. (2023). Experimental results of reinforced concrete frames with masonry infills with and without openings under combined quasi-static in-plane and out-of-plane seismic loading. *Bulletin of Earthquake Engineering, 21*, 3537–3579. https://doi.org/10.1007/s10518-023-01664-4

Milijaš, A., Marinković, M., Butenweg, C., & Klinkel, S. (2024). Experimental investigation on the seismic performance of reinforced concrete frames with decoupled masonry infills: Considering in-plane and out-of-plane load interaction effects. *Bulletin of Earthquake Engineering, 22*, 7489–7546. https://doi.org/10.1007/s10518-024-02012-w

Ou, Y.-C., Nguyen, N. V. B., & Hoang, L. (2024). Cyclic behavior and pushover analysis of large scale two-bay, two-story reinforced concrete frames infilled with walls with openings. *Engineering Structures, 317*, 118663. https://doi.org/10.1016/j.engstruct.2024.118663

Sattar, S., Hulsey, A., Hagen, G., Naeim, F., & McCabe, S. (2021). Implementing the performance-based seismic design for new reinforced concrete structures: Comparison among ASCE/SEI 41, TBI, and LATBSDC. *Earthquake Spectra, 37*(3), 2150–2173. https://doi.org/10.1177/8755293020981968

Shendkar, M. R., Kontoni, D.-P. N., Işık, E., Mandal, S., Maiti, P. R., & Harirchian, E. (2022). Influence of masonry infill on seismic design factors of reinforced-concrete buildings. *Shock and Vibration, 2022*, 5521162. https://doi.org/10.1155/2022/5521162

Wang, F., Zhao, K., Zhang, J., & Yan, K. (2021). Influence of different types of infill walls on the hysteretic performance of reinforced concrete frames. *Buildings, 11*(7), 310. https://doi.org/10.3390/buildings11070310

Zine, A., Kadid, A., & Zatar, A. (2021). Effect of masonry infill panels on the seismic response of reinforced concrete frame structures. *Civil Engineering Journal, 7*(11). https://doi.org/10.28991/cej-2021-03091764

DOI: https://doi.org/10.47667/ijpasr.v7i1.488